



# Planning and dosimetric evaluation of three total body irradiation techniques: Standard SSD VMAT, Extended SSD VMAT and Extended SSD Field-in-Field

Mert Cananoglu<sup>1</sup> · Pervin Hurmuz<sup>1</sup> · Mete Yeginer<sup>1</sup> · Gokhan Ozyigit<sup>1</sup>

Received: 5 April 2022 / Accepted: 1 October 2022 / Published online: 21 October 2022  
© The Author(s), under exclusive licence to Springer-Verlag GmbH Germany, part of Springer Nature 2022

## Abstract

The aim of this study was to dosimetrically compare three total body irradiation (TBI) techniques which can be delivered by a standard linear accelerator, and to deduce which one is preferable. Specifically, Extended Source to Surface Distance (SSD) Field-in-Field (FiF), Extended SSD Volumetric Modulated Arc Therapy (VMAT), and Standard SSD VMAT TBI techniques were dosimetrically evaluated. Percent depth dose and dose profile measurements were made under treatment conditions for each specified technique. After having generated treatment plans with a treatment planning system (TPS), dose homogeneity and critical organ doses were investigated on a Rando phantom using radiochromic films and optically stimulated luminescence dosimeters (OSLDs). TBI dose of 12 Gy in six fractions was prescribed for each technique. The gamma index (5%/5 mm) was used for the analysis of radiochromic films. Passing rates for Extended SSD FiF, Extended SSD VMAT and Standard SSD VMAT techniques were found to be 90%, 87% and 94%, respectively. OSLD measurements were within  $\pm 5\%$  agreement with TPS calculations for the first two techniques whereas the agreement was found to be within  $\pm 3\%$  for the Standard SSD VMAT technique. TPS calculations demonstrated that mean lung doses in the first two techniques were around 8.5 Gy while it was kept around 7 Gy in Standard SSD VMAT. It is concluded that Standard SSD VMAT is superior in sparing the lung tissue while all three TBI techniques are feasible in clinical practice with acceptable dose homogeneity. In the absence of VMAT-based treatment planning, Extended SSD FiF would be a reasonable choice compared to other conventional techniques.

**Keywords** Total body irradiation · TBI techniques · Lung sparing: dosimetry

## Introduction

Total body irradiation (TBI) has long been used as the conditioning regimen for bone marrow transplantation (BMT) for diseases such as lymphoma, aplastic anemia, multiple myeloma and leukaemia. TBI suppresses the immune system of the patient by destroying bone marrow cells; thus, it prepares the host for BMT and enhances the antitumor effect of chemotherapy (Khan and Gibbons 2014; Perez et al. 2019).

Target volume for TBI is the entire bone marrow and body, thus there are some limitations for treatment planning and delivering homogenous radiation doses (Mayles 2007).

The most common TBI delivery methods are anteroposterior (AP)/posteroanterior (PA) and opposed bilateral beam techniques. In these conventional techniques patient and the beams are kept stationary and source-to-surface distance (SSD) is extended to 200–600 cm to completely cover the patient body. Prescribed doses are delivered to a point to the body at the depth of the umbilicus (Khan and Gibbons 2014; Perez et al. 2019). It is known that the lungs are the dose-limiting organ, due to high risk of TBI-induced interstitial pneumonitis with high pulmonary doses (Low et al. 1998; Buchali et al. 2000; Van Dyk et al. 1986). According to the American Association of Physicists in Medicine (AAPM) Report No. 17 dose uniformity of  $\pm 10\%$  is considered acceptable while the lung dose is kept below 80%–85% of the treatment dose. Moreover, the dose to more than half of the lung volume should not exceed the treatment dose (Van Dyk et al. 1986; Penney et al. 1994).

✉ Pervin Hurmuz  
phurmuz@yahoo.com; pervin.hurmuz@hacettepe.edu.tr

<sup>1</sup> Department of Radiation Oncology, Faculty of Medicine, Hacettepe University, 06100 Ankara, Turkey

Computed tomography (CT)-based treatment planning systems (TPSs) provide detailed volumetric information and enable more accurate dose distributions compared with conventional radiotherapy methods. For instance, Volumetric Modulated Arc Therapy (VMAT) may also be used for delivering TBI at Standard SSD of approximately 100 cm. (Perez et al. 2019; Peters et al. 2015; Wong et al. 2018).

Dosimetric evaluation of TBI techniques should be performed before their clinical use. It is noted, however, that dosimetric data obtained for standard treatment fields at the Standard SSD used in conventional radiotherapy applications are not valid for extended SSDs ( $> 300$  cm) and large fields ( $40 \times 40$  cm<sup>2</sup>) used in TBI. Therefore, depth dose distribution and dose profile measurements should be performed under TBI treatment conditions (Perez et al. 2019; Wong et al. 2018). In cases where the homogeneity (in other words: flatness) of the measured dose profile is not within the desired range of  $\pm 10\%$ , compensators are used that were designed to flatten the beam (Mayles et al. 2007; Briot et al. 1990; Podgorsak 2005).

In complicated radiotherapy applications such as TBI, dose homogeneity should be verified depending on parameters such as large treatment area, irregularity in body contours and high-dose heterogeneity. To consider a treatment plan feasible, the difference between calculated and measured dose values should be within  $\pm 5\%$  (Khan and Gibbons 2014; Van Dyk et al. 1986). To our knowledge, this is the first dosimetric study comparing TBI techniques in terms of dose homogeneity.

## Materials and methods

The dosimetric evaluation of the three TBI techniques was performed with a Versa HD linear accelerator (Elekta Oncology Systems, Crawley, UK) and a Raystation TPS v8A (RaySearch Laboratories, Stockholm, Sweden) at Hacettepe University in Ankara, Turkey. The TBI techniques were Extended SSD Field-in-Field (FiF), Extended SSD VMAT and Standard SSD VMAT, which will be explained in detail in the following parts. The purpose of selecting these three techniques was to avoid the use of patient-specific dose modulation equipment thus avoiding the risk of error, further workload and increased setup time (Buchali et al. 2000; Van Dyk et al. 1986; Penney et al. 1994; Peters et al. 2015).

In TBI techniques involving Extended SSD, Percent Depth Doses (PDDs) should be measured under treatment conditions and compared with standard data. Consequently, in the present study PDDs were measured under standard conditions (SSD = 100 cm, collimator opening  $10 \times 10$  cm<sup>2</sup>); extended SSD conditions (SSD = 180 cm, collimator opening  $40 \times 40$  cm<sup>2</sup>) and conventional TBI conditions (SSD = 350 cm, collimator opening  $40 \times 40$  cm<sup>2</sup>).

The PDD measurements were performed using a PTW 34001 0.35 cc parallel plate ionization chamber and RW3 solid water phantoms. The ionization chambers were calibrated regularly in primary standard dosimetry laboratories. To precisely determine the depth of dose maximum ( $d_{\max}$ ), measurements were made at 1 mm intervals until reaching a depth of 2 cm. The rest of the measurements until a depth of 15 cm were made with 1 cm intervals. The PDD readings were normalized to the dose at  $d_{\max}$ . Dose profile measurements were made under treatment conditions using a PTW 30010 0.6 cc cylindrical ionization chamber and RW3 solid water phantoms at a depth of 10 cm. The dose profile readings at 350 cm Source to Chamber Distance (SCD) were made at 10 cm intervals in a rather homogeneous part of the profile; in contrast, in the penumbra region measurements were made at 1 cm intervals. As of 180 cm SCD, profile measurements were made at 5 cm intervals, while measurements in the penumbra region were made at 1 cm intervals. The data were then normalized to the dose at central axis.

In the treatment planning process, first a CT-simulation of an anthropomorphic phantom was performed with slice thickness of 5 mm. After that, planning target volume (PTV) was defined as the body of the phantom, shrunk to 5 mm below the surface and extended 3 mm inside the lungs. The prescription dose was determined as 12 Gy in six fractions (fx) to the PTV while sparing the lung volume. A 6 MV photon beam was used for treatment plans.

In the Extended SSD FiF technique, two bilateral fields with  $45^\circ$  collimator angles were used while the SSD was 380 cm (Onal et al. 2012). To ensure dose homogeneity, two FiFs with  $0^\circ$  collimator angles were applied from each side. In these fields, lungs and high-dose areas in the head-and-neck region are blocked with multi-leaf collimators (MLCs). A Rando phantom was placed on a TBI couch with built-in plexiglass and positioned using lasers available in the treatment room. In the Extended SSD VMAT technique, while the table rotation was  $90^\circ$ , optimization was performed using four  $100^\circ$  arcs for each supine and prone position. The Rando phantom was placed on a specially made wooden table, 30 cm above the ground using the treatment room lasers (Pierce et al. 2018; Jahnke et al. 2014). In the Standard SSD VMAT technique, optimization was performed using a total of 12 full arcs. Three isocenters were placed on the head-and-neck, thorax and abdomen regions of the Rando phantom, and four full arcs were used on each of the isocenters. Plan optimization was performed in a single plan, so the dose distribution in overlap regions was considered by summation of different sub-fields from different arcs (Symons et al. 2018). The Rando phantom was placed on the conventional treatment table with the help of kV Cone Beam Computed Tomography (CBCT).

In addition to radiochromic films, to control the mid-line dose homogeneity, OSLDs were placed at different

locations in the Rando phantom and entrance and exit doses were measured (Fig. 1). Calibration of the radiochromic films was made by irradiating the film between 0 and 220 MU (Monitor Unit) to obtain a calibration curve. The data from the irradiated films were converted to absorbed dose via this calibration curve. OSLDs, on the other hand, were calibrated using solid water phantoms, at the depth of 10 cm and 100 cm SSD, irradiated by 100 MU and analyzed after 1 h. Different coefficients were assigned to measure 100 cGy at the defined depth. After the calibration process, radiochromic films and OSLDs were placed within the Rando

phantom as specified in Tables 1 and 2. For each technique the Rando phantom was irradiated twice for radiochromic film evaluation and the obtained values were compared with TPS dose distributions using gamma analysis with 5%/5 mm passing rate criteria. OSLD measurements were performed three times for each specified point and the average values were compared with the corresponding TPS data.

### Results

In Fig. 2, PDD measurements of different conditions are compared. As the SSD increases, the surface dose and the dose at the same depth increase. Dose profiles were also measured under standard conditions (SCD = 100 cm, collimator opening 40 × 40 cm<sup>2</sup>); extended SSD (SCD = 180 cm, collimator opening 40 × 40 cm<sup>2</sup>) and conventional TBI conditions (SCD = 350 cm, collimator opening 40 × 40 cm<sup>2</sup>). When the dose profiles were examined it was found that the beam flatness decreases as the SCD increases (Fig. 3). The beam flatness is found to be within 2% at 100 cm SCD,

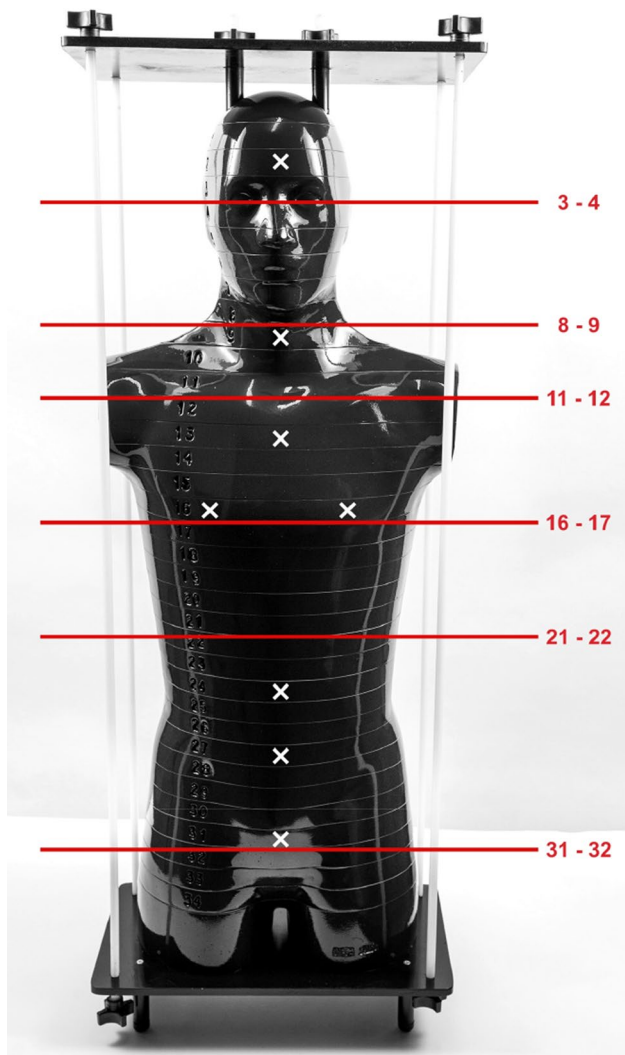


**Fig. 1** Locations of radiochromic films (red lines with slice numbers) and optically stimulated luminescence dosimeters (OSLDs) (white crosses) within the Rando phantom. Radiochromic films were placed between slices; OSLDs were placed anterior and posterior of the same slices. In the Extended SSD FiF Technique additional OSLDs were placed bilaterally on slice 11 of the Rando phantom (not shown in the figure). Also, in the Standard SSD VMAT technique, since there were two intersections of three isocenters, four additional OSLDs were placed on slices 13 and 24

**Table 1** Locations of radiochromic films between specified slices within the Rando phantom

Phantom slices	Anatomical site	Purpose of measurement
3–4	Head	Lens dose
8–9	Neck	High dose risk
11–12	Shoulder	Low dose risk
16–17	Thorax	Lung dose
21–22	Abdomen	Kidney dose
31–32	Pelvis	Gonad dose

**Table 2** Rando phantom slices where optically stimulated luminescence dosimeters (OSLDs) were placed

Phantom slice number	Anatomical site	Number of OSLDs
2	Head	2
9	Neck	2
11*	Shoulder	2
13**	Field intersection	2
16	Thorax	4
24**	Field intersection	2
27	Abdomen	2
31	Pelvis	2

\*In the Extended SSD FiF Technique, OSLDs were placed in this slice because of low-dose risk in the shoulders

\*\*Since three different isocenters were used in the Standard SSD VMAT technique, there were two junction areas. To control the dose homogeneity in these regions, OSLDs were placed in these slices

**Fig. 2** Comparison of percent depth doses (PDDs) measured at different source-to-chamber distances (SCDs) (100 cm, 180 cm, 350 cm) in a RW3 solid water phantom, and normalized to the surface dose. (Dose uncertainties were generally of the order of 1%)

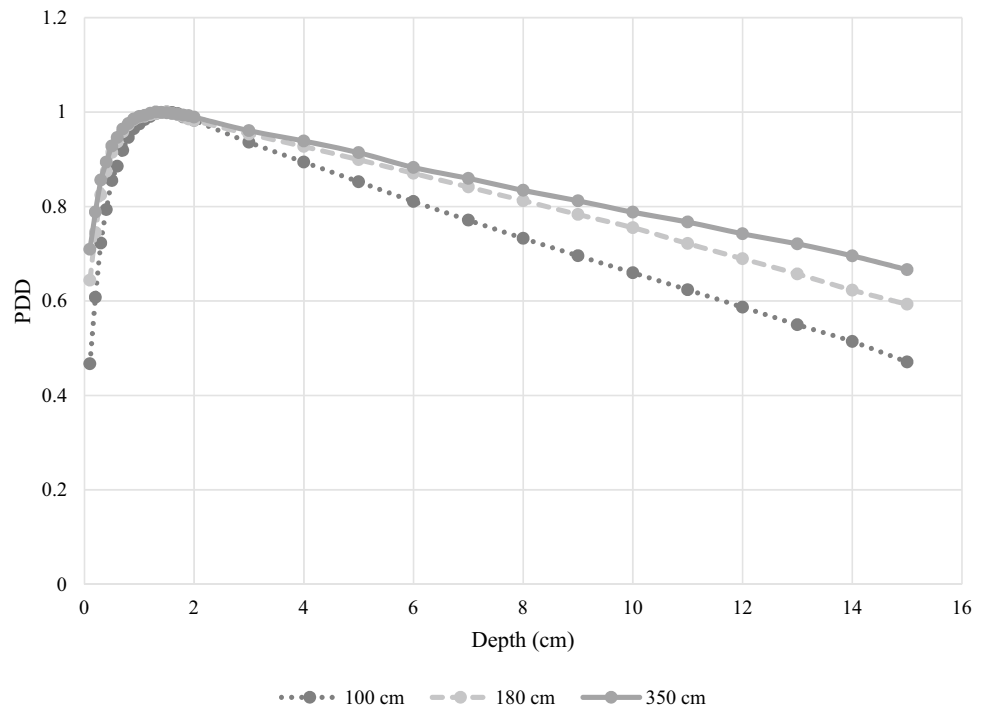
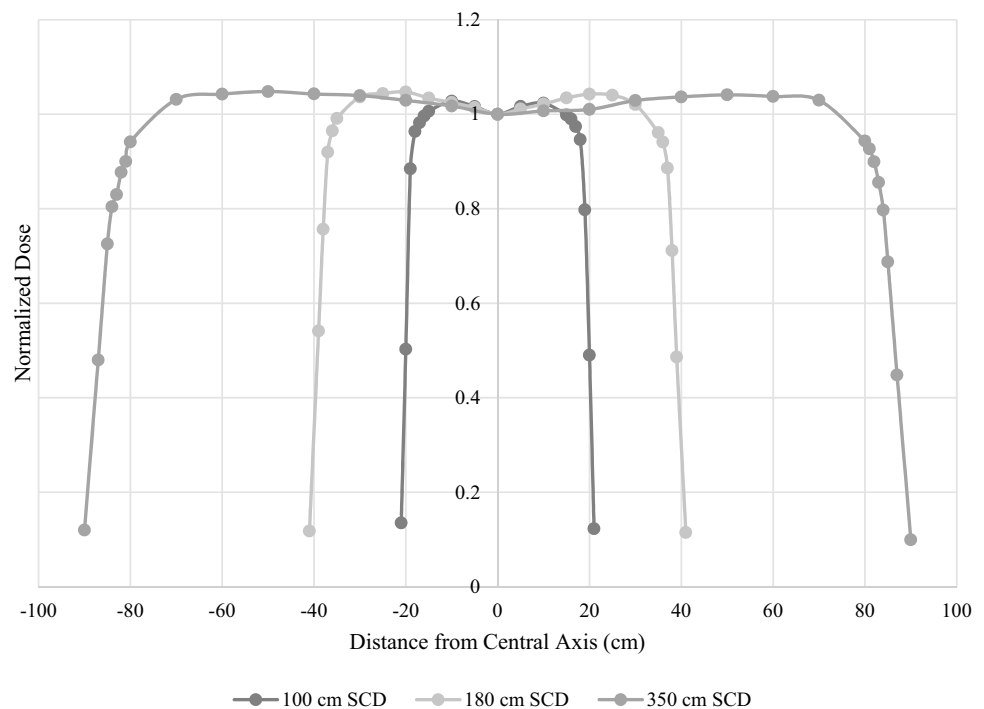


**Fig. 3** Comparison of dose profiles measured at different source-to-chamber distances (SCDs) (100 cm, 180 cm, 350 cm) in a RW3 solid water phantom. (Dose uncertainties were generally of the order of 1%)



4% at 180 cm SCD and 4.79% at 350 cm SCD. Likewise, it was found that the penumbra increased with increasing SCD. Specifically, compared to 100 cm SCD, the widths of penumbra regions increased by factors of 1.8 and 3.3 for SCDs of 180 cm and 350 cm, respectively.

Mean PTV doses in Extended SSD FiF, Extended SSD VMAT and Standard SSD VMAT techniques were 11.9,

11.8 and 12.0 Gy, respectively (Table 3). Corresponding mean lung doses, however, were 8.5 Gy, 8.6 Gy and 6.9 Gy, respectively (Table 4). It was found that the mean lung dose for Standard SSD VMAT technique was 20% lower than that obtained by the other two techniques.

After the optimization process, line doses were obtained in cranio-caudal (head to feet) direction. As seen in Fig. 4,

**Table 3** Comparison of planning target volume (PTV) doses for the three techniques in Gy

Technique	D <sub>95</sub> **	D <sub>90</sub> **	Mean dose	D <sub>50</sub> **	D <sub>10</sub> **	D <sub>1</sub> **	D <sub>5cc</sub> ***	HI
I	9.7	11.0	11.9	11.5	12.4	13.2	14.9	0.89
II	9.7	10.8	11.8	11.6	12.8	13.6	14.8	0.84
III	11.4	11.8	12.1	12.0	12.3	12.9	13.8	0.96

\*I: Extended SSD FiF Technique, II: Extended SSD VMAT Technique, III: Standard SSD VMAT Technique, HI: Homogeneity Index (D<sub>90</sub>/D<sub>10</sub>)

\*\*D<sub>95</sub>, D<sub>90</sub>, D<sub>50</sub>, D<sub>10</sub> and D<sub>1</sub> are the doses received by 95%, 90%, 50%, 10% and 1% of the PTV respectively

\*\*\*D<sub>5cc</sub> is defined as the minimal dose received by the highest irradiated volume of 5 cc

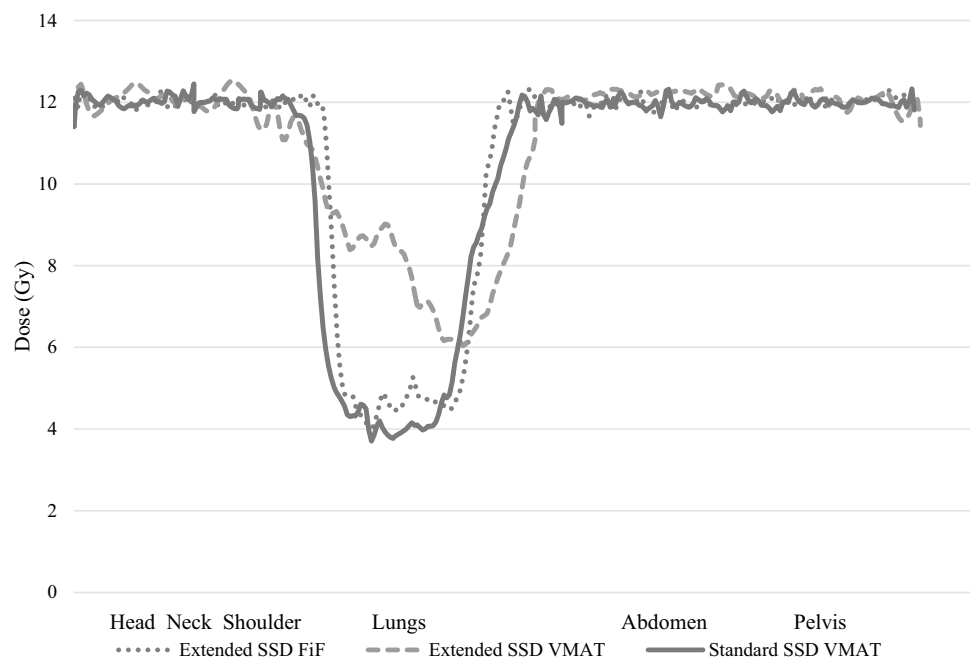
**Table 4** Treatment plan-based lung doses in Gy

Technique	D <sub>99</sub> **	D <sub>95</sub> **	Mean dose	D <sub>50</sub> **	D <sub>2</sub> **	D <sub>1</sub> **
I	6.0	6.4	8.5	8.5	10.9	11.3
II	6.1	6.7	8.6	8.4	11.7	12.0
III	3.2	3.5	6.9	6.6	11.5	11.8

\*I: Extended SSD FiF Technique, II: Extended SSD VMAT Technique, III: Standard SSD VMAT Technique

\*\*D<sub>99</sub>, D<sub>95</sub>, D<sub>50</sub>, D<sub>2</sub> and D<sub>1</sub> are the doses received by 99%, 95%, 50%, 2% and 1% of the lungs, respectively

**Fig. 4** Comparison of cranio-caudal line doses of Total Body Irradiation (TBI) plans for Extended SSD FiF, Extended SSD VMAT, and Standard SSD VMAT



except for the lungs, PTV homogeneities of treatment plans were close to each other. Even though the mean lung doses of both the Extended SSD FiF and Extended SSD VMAT techniques are similar in V5 (total lung volume that receives 5 Gy) is higher in the latter technique. In Extended SSD FiF technique all tissues around the lung receive less than 90% of the treatment dose. In the Extended SSD VMAT technique, the low-dose region (where the prescription dose could not be achieved) was formed only in the anterior and posterior

of the lungs. In the Standard SSD VMAT technique, on the other hand, there was no low-dose region around the lungs, and most of the lung volume was kept within the 50% isodose curve.

According to the gamma analysis of radiochromic film doses, the passing rate of the treatment plan prepared with the Extended SSD FiF technique was found to be 90% on average, while in the Extended SSD VMAT technique this rate was 87% on average. Finally, in the Standard

SSD VMAT technique, the passing rate was 94% on average (Table 5). Moreover, in the Extended SSD FiF and Extended SSD VMAT techniques the differences between OSLD measurements and TPS calculations were in the range of  $\pm 5\%$ . In the Standard SSD VMAT technique, these differences were within  $\pm 3\%$  (Tables 6, 7).

## Discussion

TBI has long been applied via conventional methods such as bilateral or AP/PA techniques. The increasing popularity of VMAT has raised the question whether TBI could be also implemented with VMAT. TBI with conventional linacs at standard SSD is not yet prevalent although, due to large treatment field and multiple overlapping arcs, this technique is of interest. In the present study the three TBI techniques

**Table 5** Gamma analysis of radiochromic film doses in percentage

Phantom slices	Extended SSD FiF	Extended SSD VMAT	Standard SSD VMAT
3–4	89.30 $\pm$ 0.80	88.10 $\pm$ 0.60	93.35 $\pm$ 0.45
9–10	89.15 $\pm$ 0.15	87.60 $\pm$ 1.00	93.30 $\pm$ 0.40
11–12	89.75 $\pm$ 0.35	85.65 $\pm$ 0.55	95.35 $\pm$ 0.15
16–17	86.00 $\pm$ 0.20	82.45 $\pm$ 0.35	87.90 $\pm$ 0.30
25–18	90.25 $\pm$ 0.25	86.95 $\pm$ 0.85	91.00 $\pm$ 0.20
31–32	89.10 $\pm$ 0.60	89.25 $\pm$ 0.55	94.95 $\pm$ 0.15

**Table 6** Optically stimulated luminescence dosimeter (OSLD) readings in Gy

Phantom slice number	Extended SSD FiF		Extended SSD VMAT		Standard SSD VMAT	
	Right	Left	Front	Back	Front	Back
2	12.4 $\pm$ 0.3	12.5 $\pm$ 0.4	11.6 $\pm$ 0.2	11.2 $\pm$ 0.2	10.7 $\pm$ 0.4	11 $\pm$ 0.3
9	12.1 $\pm$ 0	12.3 $\pm$ 0.1	11.4 $\pm$ 0.2	11.4 $\pm$ 0.2	11.1 $\pm$ 0.9	11.4 $\pm$ 0.8
11*	12.5 $\pm$ 0.1	12.3 $\pm$ 0.1	–	–	–	–
13**	–	–	–	–	11.4 $\pm$ 0.6	11.7 $\pm$ 0.2
16	7.4 $\pm$ 0.1	7.3 $\pm$ 0	7.9 $\pm$ 0.1	7.6 $\pm$ 0.4	11.9 $\pm$ 0.5	12.3 $\pm$ 0.7
24**	–	–	–	–	11.5 $\pm$ 0.3	11.7 $\pm$ 0.2
27	12.2 $\pm$ 0.2	12.2 $\pm$ 0.2	11.5 $\pm$ 0.1	11.1 $\pm$ 0.2	11.6 $\pm$ 0.5	11.9 $\pm$ 0.2
31	12.5 $\pm$ 0.3	12.6 $\pm$ 0.3	11.2 $\pm$ 0.1	11 $\pm$ 0	11.7 $\pm$ 0.3	12 $\pm$ 0.3

\*In the Extended SSD FiF Technique, OSLDs were placed in this slice because of low-dose risk in the shoulders

\*\*Since three different isocenters were used in the Standard SSD VMAT technique, there were two junction areas. To control the dose homogeneity in these regions, OSLDs were placed in these slices

**Table 7** Percentage differences between optically stimulated luminescence dosimeter (OSLD) readings and corresponding treatment planning system (TPS) values

Phantom slice number	Extended SSD FiF		Extended SSD VMAT		Standard SSD VMAT	
	Right	Left	Front	Back	Front	Back
2	– 1.08	1.52	4.87	3.28	2.44	2.87
9	– 2.16	1.95	2.73	4.14	1.91	1.88
11*	– 1.28	– 4.99	–	–	–	–
13**	–	–	–	–	– 0.94	– 2.89
16	3.14	4.58	– 0.64	3.93	– 0.76	– 1.22
24**	–	–	–	–	0.90	2.33
27	– 1.51	– 1.54	5.07	2.66	– 2.97	– 1.29
31	– 1.44	1.02	4.81	4.93	2.76	2.60

\*In the Extended SSD FiF Technique, OSLDs were placed in this slice because of low-dose risk in the shoulders

\*\*Since three different isocenters were used in the Standard SSD VMAT technique, there were two junction areas. To control the dose homogeneity in these regions, OSLDs were placed in these slices

most frequently used in modern radiotherapy were compared and their clinical feasibility evaluated. To the best of the authors' knowledge this is the first study comparing TBI techniques using the same linac and TPS.

In conventional TBI applications, the width of the central treatment field with homogeneous dose distribution must be measured at the treatment distance. It is emphasized that the applicable field width cannot be obtained directly by just proportionally enlarging the light field used to define field size, because the penumbra region at the field edges results in an applicable area width which is always smaller than the light field width. When the collimator was opened  $40 \times 40$  cm<sup>2</sup> and turned 45°, the diagonal lengths of the light field (i.e. 50% isodose curve) and the central region (i.e. 90% isodose curve) at 350 cm SCD were measured as 198 cm and 162 cm, respectively. Dose profiles were measured at 180 cm and 350 cm SCD, and the beam flatness was found to be 4% and 4.79%, respectively. Hoseinnezhad et al. (2020) similarly found a profile flatness of 4.59% at 312 cm SSD. Since the measured dose profiles in both SCDs provide  $\pm 10\%$  dose homogeneity, no flattening compensators were required in the study by Hoseinnezhad et al. (2020).

In addition to the dose profile, PDDs should also be examined under treatment conditions in TBI techniques using extended SSD. In the present study, PDD was measured at 350 cm SSD for the Extended SSD FiF technique and the  $d_{\max}$  was found at 1.3 cm. As shown in Fig. 2, compared to the standard SSD, the surface dose increased from 47 to 70%; at a depth of 10 cm the PDD was higher (79% instead of 66%) (Fig. 1). Since the surface dose was low, a beam spoiler was used in this technique. In the measurements made with plexiglass, the surface dose raised up to 98% of the prescription dose, while the dose at 10 cm depth was found to be 77%. Onal et al. (2012) reported a similar surface dose with plexiglass of 97.5% of the prescription dose. For the Extended SSD VMAT technique, on the other hand, PDD was measured at 180 cm SSD and compared to 100 cm and no difference was observed in the  $d_{\max}$ . This result is compatible with the results of Pierce et al. (2018). In the present study, compared to the standard SSD, the surface dose increased from 47 to 64%, and at a depth of 10 cm, PDD increased from 66 to 76%. When the dose profile at 180 cm SCD was examined, the area within the 90% isodose curve was found to be  $74 \times 74$  cm<sup>2</sup>. Pierce et al. (2018) used 175 cm SSD and presented the dose profile only graphically where the field dimension was smaller than  $80 \times 80$  cm<sup>2</sup>.

In the treatment plan prepared with the Extended SSD FiF technique, the mean lung dose was reduced to 70% of the prescribed dose and high-dose areas within the lung was avoided. For comparison, in the study of Onal et al. (2012) the mean lung dose was 79.2% of the treatment dose. In the Extended SSD VMAT technique, while the table rotation was 90°, eight 100° arcs were used in the supine and prone

position, and the lung dose was similarly reduced to 70% of the treatment dose. Note that Pierce et al. (2018) did not need to protect any organ since their study was on low-dose TBI. In the present study, for the Standard SSD VMAT technique a treatment plan was created using twelve full arcs with three isocenters placed on the head-and-neck, thorax and abdomen regions, and the mean lung dose was reduced to 60% of the treatment dose. In the study of Symons et al. (2018), this value was 63%. In the present study, the homogeneity indices ( $D_{90}/D_{10}$ ) of Extended and Standard SSD techniques were found to be 89%, 84% and 96%, respectively.

The remarkable advantage of the Standard SSD VMAT technique over the extended SSD techniques is the reduced mean lung dose while the prescribed dose is homogeneously delivered to the target volume. Van Dyk et al. (1981, 1982) have shown that a 5% dose increase in the lungs escalate the risk of radiation pneumonitis by 20%. They found that for single fraction treatments, the incidence of radiation pneumonitis begins at 7.5 Gy, and the risk reaches 5% at 8.2 Gy. Above this dose the complication curve rises sharply, reaching 50% at 9.3 Gy and 95% at 10.6 Gy. Clift et al. (1990) compared 15.75 Gy (2.25 Gy/tx) with 12 Gy (2 Gy/tx) TBI doses, and showed that relapse probabilities were 13% and 35%, respectively. These authors also found that high-dose TBI caused an increase in pneumonitis rate (Clift 1990). Therefore, the low mean lung dose (6.9 Gy) obtained in the present study for the Standard SSD VMAT technique allows the treatment dose to be escalated for selected cases.

One of the critical disadvantages of the Standard SSD VMAT technique is the fact that the dose rates are variable. A recent study by Kobyzeva et al. (2021) has shown that the dose rates achieved in the present study with VMAT have not caused any increase in toxicity and first reports show promising results (Hoeben et al. 2022). The second disadvantage is the risk of low/high dose that may occur at field junctions due to the use of more than one isocenter. Since three isocenters were used in the present study, two junctions were formed. These intersection areas correspond to the 13th and 24th slices of the Rando phantom. Dose distribution was examined by placing OSLDs on the anterior and posterior regions of these slices, and no dose heterogeneity was observed (Table 7).

Since the present study was performed using a Rando phantom the main limitation was the lack of extremities of the body. For the Extended SSD techniques, field size would be sufficient to encompass the body. In contrast, for the Standard SSD VMAT technique at least three more isocenters would be needed to irradiate the whole body. To do that a second CT on the feet first supine (FFS) orientation would be combined with the head first supine (HFS) CT and optimization would then be performed. It is noted that a novel technique has recently been introduced by Losert et al. (2019) who applied a rotational couch top, which supersedes

the need of repositioning the patient between HFS and FFS orientations.

## Conclusions

In the present dosimetric study, it was found that Standard SSD VMAT can replace Extended SSD in TBI avoiding commissioning and patient-based dose modulation equipment. An additional advantage over other techniques is the fact that Standard SSD VMAT can be applied in a standard linear accelerator room. Although it is more laborious in treatment planning and delivery phases compared to the other two investigated techniques, because more than one isocenter must be used, it allows for a high-dose homogeneity with lower lung doses. Moreover, in the Standard SSD VMAT technique the irradiation can take place on a conventional treatment table involving kV CBCT and, as a result, the risk of human-based errors is reduced. Thus, in each fraction, the treatment position can be precisely repeated and the prescribed dose can be accurately delivered.

In conclusion all three TBI techniques appear to be feasible to be used in the clinics with appropriate dose homogeneity. However, the Standard SSD VMAT technique was found to be more practical and better in sparing the lung tissue. In the absence of VMAT, Extended SSD FiF would be a reasonable choice compared to the conventional technique, because the planning process is much less tedious than in the conventional TBI technique.

**Acknowledgements** This study was supported by Hacettepe University Research Grant Project TYL-2019-18416.

**Author contribution** M.C. and P.H. designed the study and wrote the main manuscript, M.Y. and G.O reviewed the manuscript and interpreted the results.

**Funding** This study is supported by Hacettepe University Research Grant Project: TYL-2019-18416.

## Declarations

**Conflict of interests** The authors declare no competing interests.

**Ethics statements** Not applicable (This is a dosimetric study without patient data).

## References

- Briot E, Dutreix A, Bridier A (1990) Dosimetry for total body irradiation. *Radiother Oncol* 18:16–29. [https://doi.org/10.1016/0167-8140\(90\)90175-v](https://doi.org/10.1016/0167-8140(90)90175-v)
- Buchali A, Feyer P, Groll J, Massenkeil G, Arnold R, Budach V (2000) Immediate toxicity during fractionated total body irradiation as conditioning for bone marrow transplantation. *Radiother Oncol* 54(2):157–162
- Clift R, Buckner C, Appelbaum F, Bearman S, Petersen F, Fisher LD, Anasetti C, Beatty P, Bensinger WI, Doney K (1990) Allogeneic marrow transplantation in patients with acute myeloid leukemia in first remission: a randomized trial of two irradiation regimens. *Blood* 76(9):1867–1871. <https://doi.org/10.1182/blood.v76.9.1867.bloodjournal7691867>
- Hoeben BAW, Pazos M, Seravalli E, Bosman ME, Losert C, Albert MH et al (2022) ESTRO ACROP and SIOPE recommendations for myeloablative Total Body Irradiation in children. *Radiother Oncol* 173:119–133
- Hoseinnezhad E, Geraily G, Esfahani M, Farzin M, Gholami S (2020) Comparison of calculated and measured basic dosimetric parameters for total body irradiation with 6- and 18-MV photon beams. *J Radiother Pract* 24:1–5
- Jahnke A, Jahnke L, Molina-Duran F, Ehmann M, Kantz S, Steil V, Wenz F, Glatting G, Lohr F, Polednik M (2014) Arc therapy for total body irradiation: a robust novel treatment technique for standard treatment rooms. *Radiother Oncol* 110(3):553–557. <https://doi.org/10.1016/j.radonc.2013.12.009>
- Khan FM, Gibbons JP (2014) Khan's the physics of radiation therapy. Wolters Kluwer, Philadelphia
- Kobyzeva D, Shelikhova L, Loginova A, Kanestri F, Tovmasyan D, Maschan M, Khismatullina R, Ilushina M, Baidildina D, Myakova N, Nechesnyuk A (2021) Optimized conformal total body irradiation among recipients of TCR $\alpha\beta$ /CD19-depleted grafts in pediatric patients with hematologic malignancies: single-center experience. *Front Oncol*. <https://doi.org/10.3389/fonc.2021.785916>
- Losert C, Shpani R, Kiefling R, Freislederer P, Li M, Walter F, Niyazi M, Reiner M, Belka C, Corradini S (2019) Novel rotatable tabletop for total-body irradiation using a linac-based VMAT technique. *Radiat Oncol* 14(1):244. <https://doi.org/10.1186/s13014-019-1445-3>
- Low DA, Harms WB, Mutic S, Purdy JA (1998) A technique for the quantitative evaluation of dose distributions. *Med Phys* 25(5):656–661
- Mayles P, Nahum AE, Rosenwald J-C (2007) Handbook of radiotherapy physics: theory and practice. Taylor & Francis, New York
- Onal C, Sonmez A, Arslan G, Sonmez S, Efe E, Oymak E (2012) Evaluation of field-in-field technique for total body irradiation. *Int J Radiat Oncol Biol Phys* 83(5):1641–1648
- Penney DP, Sieman DW, Rubin P, Maltby K (1994) Morphological correlates of fractionated radiation of the mouse lung: early and late effects. *Int J Radiat Oncol Biol Phys* 29(4):789–804
- Perez CA, Halperin EC, Brady LW (2019) Perez and Brady's principles and practice of radiation oncology. Wolters Kluwer Health/Lippincott Williams & Wilkins, Philadelphia
- Peters M, Taylor B, Turner E (2015) An evidence-based review of total body irradiation. *J Med Imaging Radiat Sci* 46(4):442–449
- Pierce G, Balogh A, Frederick R, Gordon D, Yarschenko A, Hudson A (2018) Extended SSD VMAT treatment for total body irradiation. *J Appl Clin Med Phys* 20(1):200–211
- Podgorsak EB (2005) Radiation oncology physics: a handbook for teachers and students. IAEA, Vienna
- Symons K, Morrison C, Parry J, Woodings S, Zissiadis Y (2018) Volumetric modulated arc therapy for total body irradiation: a feasibility study using Pinnacle3 treatment planning system and Elekta Agility™ linac. *J Appl Clin Med Phys* 19(2):103–110
- Van Dyk J, Keane TJ, Kan S, Rider WD, Fryer CJH (1981) Radiation pneumonitis following large single dose irradiation: a re-evaluation based on absolute dose to lung. *Int J Radiat Oncol Biol Phys* 7(4):461–467
- Van Dyk J, Keane TJ, Rider WD (1982) Lung density as measured by computerized tomography: implications for radiotherapy. *Int J Radiat Oncol Biol Phys* 8(8):1363–1372



- Van Dyk J, Glavin JM, Glasgow GP (1986) AAPM's TG-29 protocol for the physical aspects of total and half body photon irradiation. American Association of Physicists in Medicine
- Wong JYC, Filippi AR, Dabaja BS, Yahalom J, Specht L (2018) Total body irradiation: guidelines from the International Lymphoma Radiation Oncology Group (ILROG). *Int J Radiat Oncol Biol Phys* 101(3):521–529

Springer Nature or its licensor (e.g. a society or other partner) holds exclusive rights to this article under a publishing agreement with the author(s) or other rightsholder(s); author self-archiving of the accepted manuscript version of this article is solely governed by the terms of such publishing agreement and applicable law.

**Publisher's Note** Springer Nature remains neutral with regard to jurisdictional claims in published maps and institutional affiliations.